European School of Antennas
“High-frequency techniques and Travelling-wave antennas”

General Properties of Planar Leaky-Wave Antennas

Giampiero Lovat

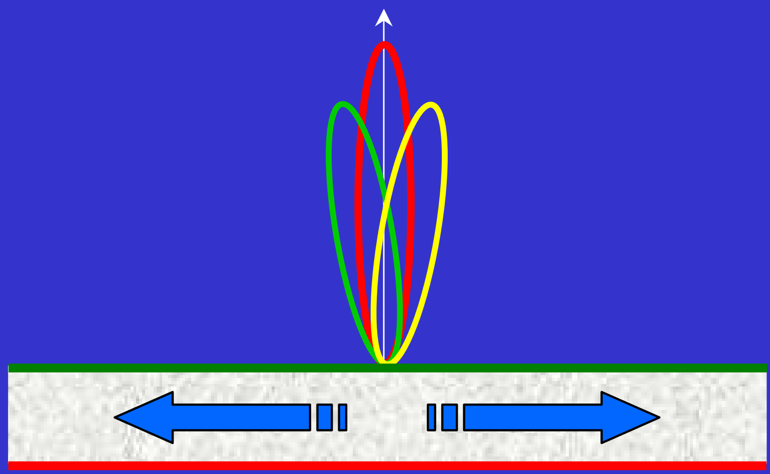

“La Sapienza” University of Rome

Roma, 24th February 2005

Introduction (1)

- Leaky-wave antennas (LWAs) belong to the traveling-wave antenna family

  Radiation occurs from a traveling wave with a complex wavenumber $\beta - j\alpha$

- Phase constant β controls the scan angle
  Attenuation constant α controls the beamwidth

  Both are dependent on the geometry of the LWA structure

- LWAs made in printed-circuit fashion enjoy the advantages of:
  - being low profile
  - having structure simplicity
  - being compatible with easy integration

Introduction (2)

- Depending on the geometry, there are *two* types of planar LWAs:

Uniform planar LWAs

uniform guiding structure which supports a leaky wave

Periodic planar LWAs

open periodic structure in which radiation is due to the excitation of a leaky Floquet mode that has (at least) *one axially fast spatial harmonic*

- From the nature of the traveling wave, there is another classification:
  - 1D LWA radiates from a wave traveling in a fixed direction
  - 2D LWA radiates from a wave traveling radially along a planar surface

One-Dimensional Uniform Dielectric Leaky-Wave Antennas

An Example of 1D Dielectric LWAs

- The antenna consists of an even number of dielectric layers above a ground plane, with a simple source inside (e.g., an infinite electric-line current)

- A simple example is a substrate-superstrate configuration:

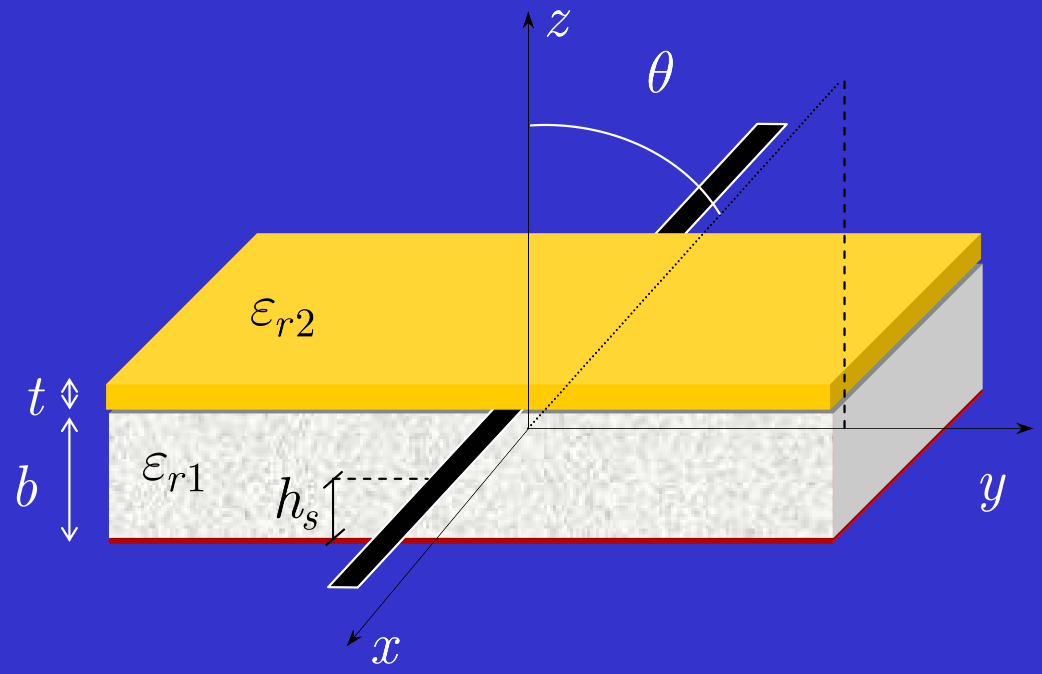

A Bit of History… (1)

- In 1985, it was proposed by Alexòpoulos and Jackson as a printed-circuit antenna with a large gain and narrow beam at $\theta = \theta_p$ when the following conditions ("resonance conditions") are satisfied:

$$\begin{cases} k_0 b\sqrt{\varepsilon_{r1} - \sin^2\theta_p} = \pi \\ k_0 t\sqrt{\varepsilon_{r2} - \sin^2\theta_p} = \dfrac{\pi}{2} \end{cases}$$

- In fact, when $\varepsilon_{r2} \gg 1$ the gain at $\theta = \theta_p$ becomes increasingly large as $\varepsilon_{r2} \rightarrow \infty$ with a resultant decrease in beamwidth

Although providing for convenient formulas, their derivation did not by itself provide any insight into the fundamental cause of the narrow-beam phenomenon

A bit of history… (2)

- *"David Jackson had just completed his doctorate at UCLA, and Prof. Arthur Oliner invited him to present a seminar at Polytechnic of New York. Someone pointed out that an alternative explanation for the high-gain effect was in terms of a leaky mode*
- *David Jackson replied that he didn't know anything about leaky waves, but he would look into it. Later, Prof. Oliner drove him to the airport, and they arrived about 45 minutes early for the flight. While they were waiting, Jackson asked Oliner to tell him something about leaky waves and how his structure would be analyzed in those terms. Prof. Oliner did so, and Jackson took notes. They did what they could in 45 minutes and then they said goodbye*
- *Nine months later Oliner received a large envelope from Jackson containing a complete paper describing the leaky-mode explanation of the phenomenon"*

Prof. Oliner and Prof. Jackson are today widely viewed as the masters of leaky waves

A Bit of History… (3)

- Jackson and Oliner showed that the resonance gain effect may be elegantly described in terms of leaky waves

- They proved that the resonance conditions correspond to the excitation of a weakly attenuated leaky wave on the structure

- The leaky mode becomes dominant when $\varepsilon_{r2} \gg 1$ and in particular

$$\begin{aligned} &\beta \to k_0 \sin\theta_p \\ &\alpha \to 0 \end{aligned} \qquad \text{for} \quad \varepsilon_{r2} \to \infty$$

Structure Description

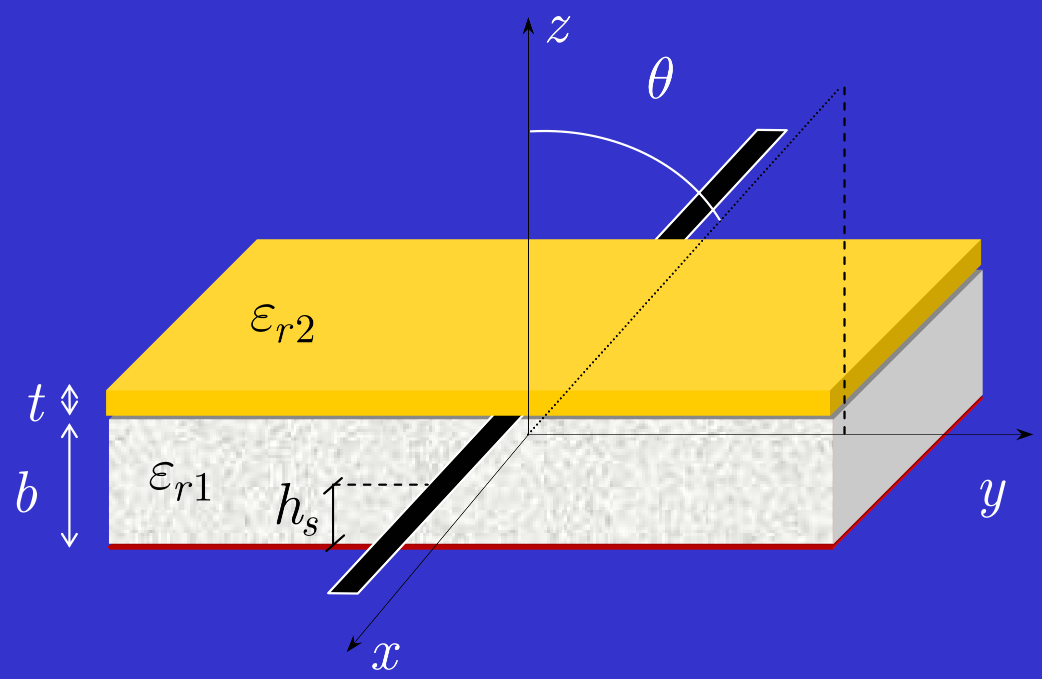

- A lossless structure is considered
- A time-harmonic behavior is assumed
- The source consists of an electric-current line placed at a height h_s above the ground which excites a purely TE field

Total Aperture and Radiated Field

- The electric field $E_x(y,0)$ on the aperture can be expressed as an inverse Fourier transform

$$E_x(y,0) = \frac{1}{2\pi}\int_{-\infty}^{+\infty} \tilde{G}_{xx}^{TE}\left(0,k_y\right)e^{-jk_y y}\mathrm{d}k_y$$

where $\tilde{G}_{xx}^{TE}\left(0,k_y\right)$ is the spectral Green's function of the problem which can be obtained in a simple closed form

- The electric far field is proportional to the Fourier transform of the aperture field, so that the radiated angular power density is

$$P(\theta) = \frac{k_0}{4\pi\eta_0}\cos^2\theta\left|\tilde{G}_{xx}^{TE}\left(0,k_0\sin\theta\right)\right|^2$$

Aperture Constituent Fields (1)

- The SGF $\tilde{G}_{xx}^{TE}\left(k_y\right)$ has both pole singularities and branch points

  pole singularities $\longrightarrow$ discrete spectrum

  branch points $\longrightarrow$ continuous spectrum

  $\downarrow$

  By means of the Sommerfeld branch cuts, proper and improper Riemann sheets can be defined

- The original integration path for the calculation of the total aperture field lies along the real axis of the complex k_y plane

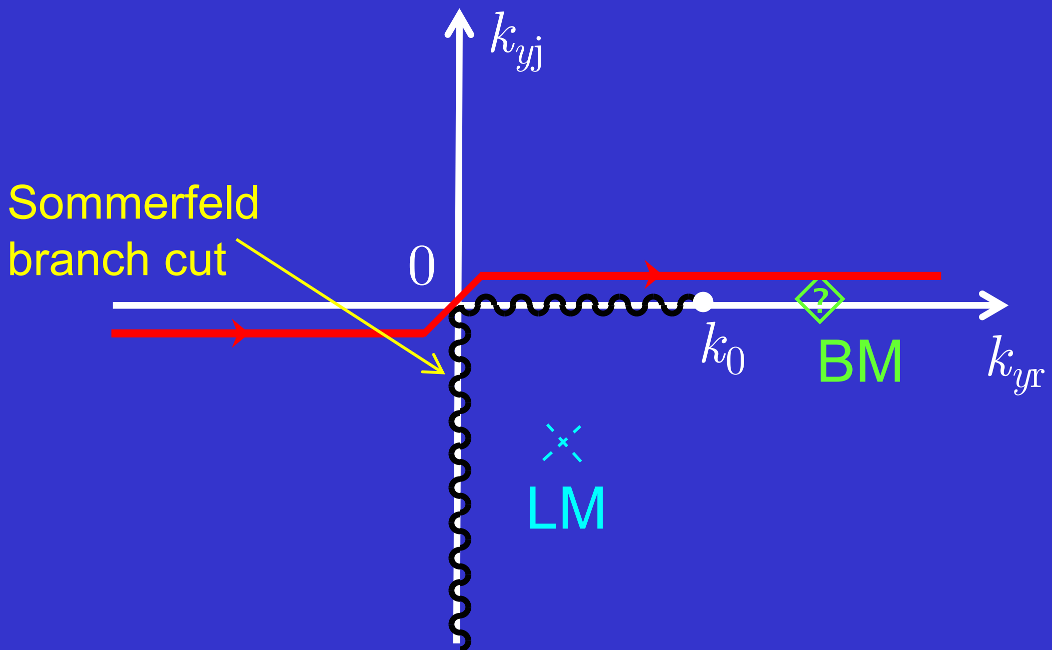

BM $\longrightarrow$ proper real bound-mode pole

LM $\longrightarrow$ improper complex leaky-mode pole

Aperture Constituent Fields (2)

- By an application of the residue theorem, the original integration path along the real axis of the k_y plane can be deformed (for $y > 0$) in the lower half plane into a path along the Sommerfeld branch cut

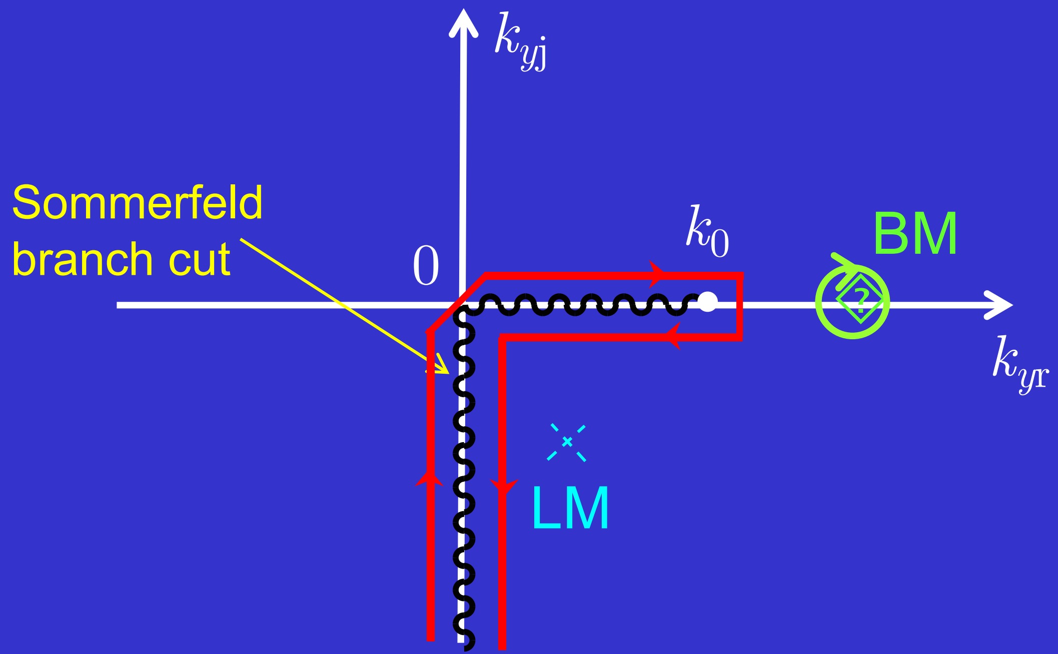

The total aperture field can be expressed as the sum of *two* terms:

$$E_x(y) = \underbrace{\frac{1}{2\pi} \int_{\text{Branch Cut}} \tilde{G}_{xx}(k_y) e^{-jk_y y} \mathrm{d}k_y}_{\text{Continuous spectrum}} - \underbrace{j \sum_i \mathrm{Res}\left[\tilde{G}_{xx}(k_{BM_i})\right] e^{-jk_{BM_i} y}}_{\text{Discrete spectrum (surface waves)}}$$

Aperture Constituent Fields (3)

- By further deforming the integration path to the steepest descent path SDP (which lies partly on the proper and partly on the improper Riemann sheet) the continuous spectrum can be expressed as the sum of other *two* contributions

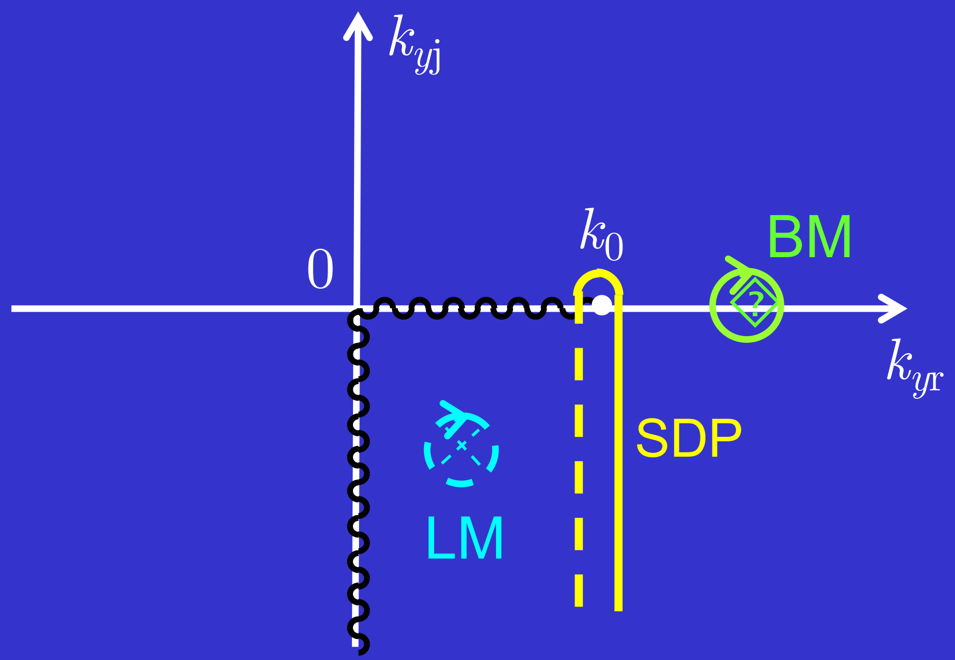

$$E_x^{CS}(y) = \underbrace{\frac{1}{2\pi}\int_{\mathrm{SDP}} \tilde{G}_{xx}(k_y)\, e^{-jk_y y}\,\mathrm{d}k_y}_{\text{Residual wave}} \underbrace{- j\sum_i \mathrm{Res}\left[\tilde{G}_{xx}(k_{LM_i})\right] e^{-jk_{LM_i} y}}_{\text{Leaky waves}}$$

Leaky-Mode Aperture and Radiation Field

- Far-field radiation pattern mainly depends on the continuous-spectrum part of the field
- When the structure is optimized according to the resonance conditions, the leaky mode with the smallest attenuation constant is dominant with respect to all the other (higher-order) leaky modes and to the residual wave

$$E_x^{CS}(y) \simeq E_x^{LM}(y) \simeq E_0 e^{-jk_{LM}|y|}$$

- The corresponding leaky-mode radiated angular power density is

$$P_{LM}(\theta) = \frac{k_0 \,|\, E_0 \,|^2}{\pi \eta_0} |\, k_{LM} \,|^2 \frac{\cos^2(\theta)}{\left| k_0^2 \sin^2\theta - k_{LM}^2 \right|^2}$$

Dispersion Curves (1)

Parameters: $\varepsilon_{r1} = 2.2$, $\varepsilon_{r2} = 55$
$b = 4.152$ mm, $t = 0.339$ mm

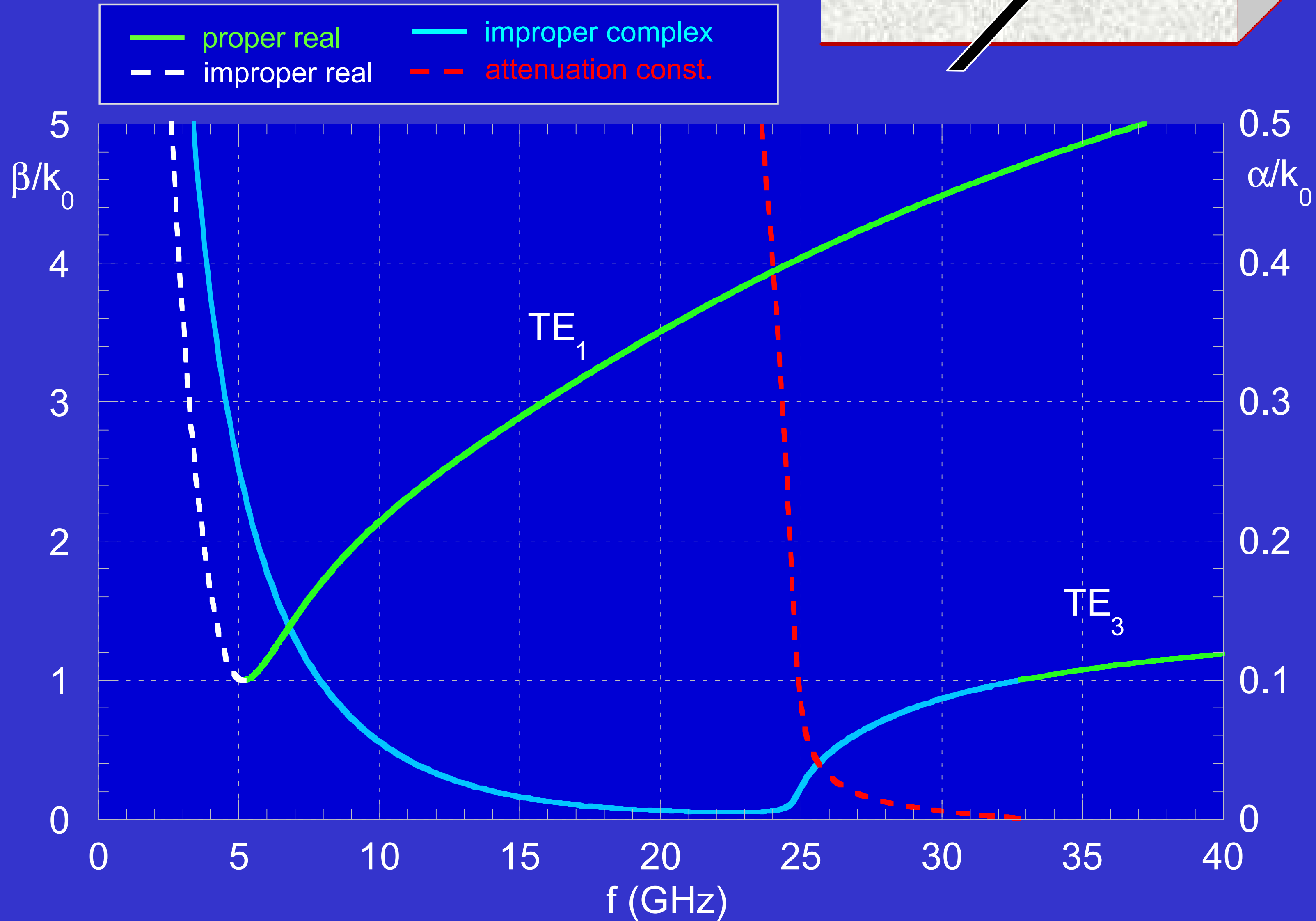

Dispersion Curves (2)

Parameters: ε_{r1} = 2.2, ε_{r2} = 55
b = 4.152 mm, t = 0.339 mm

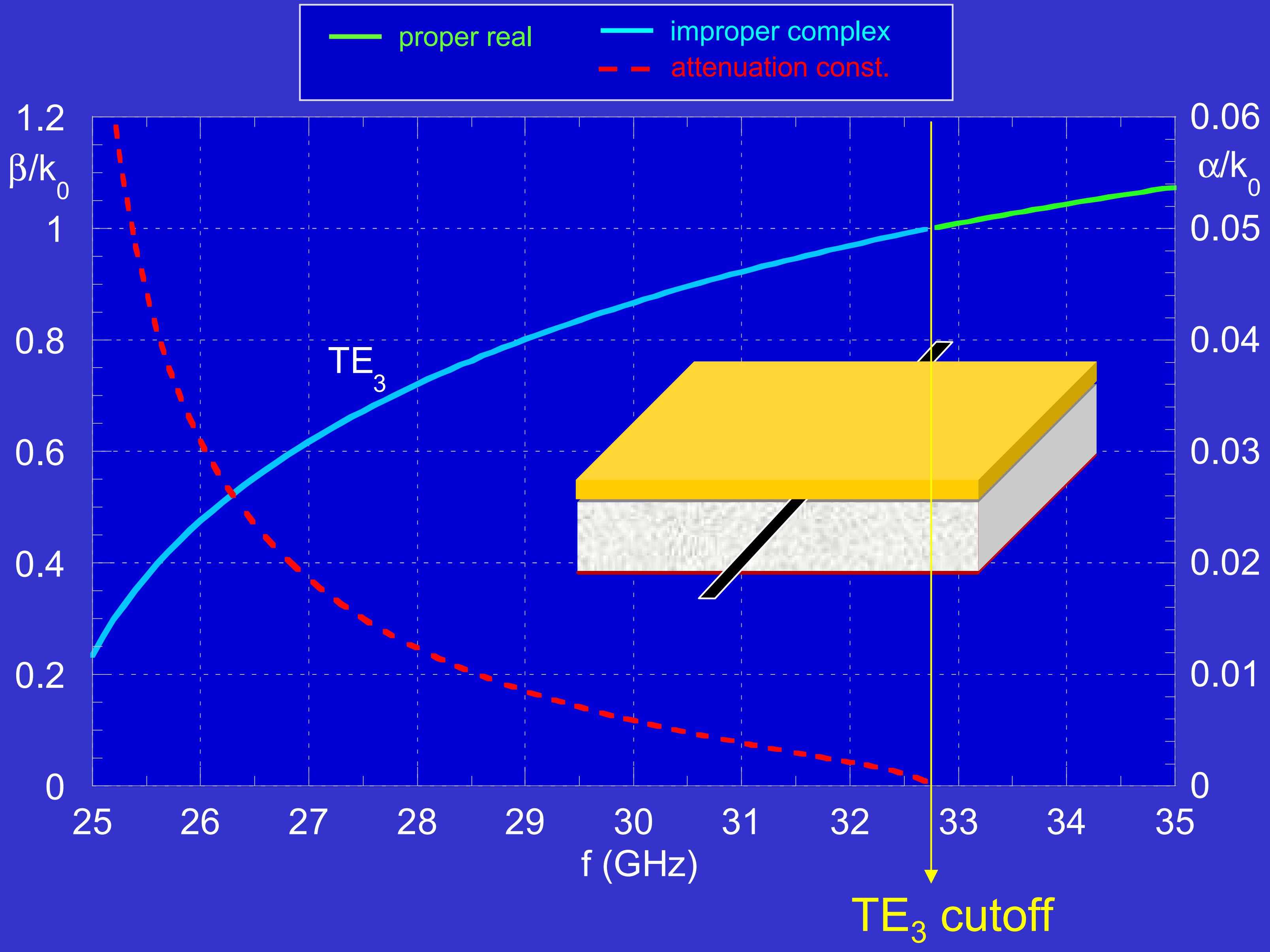

Aperture Constituent Fields

f = 30 GHz, $h_s = b/2$

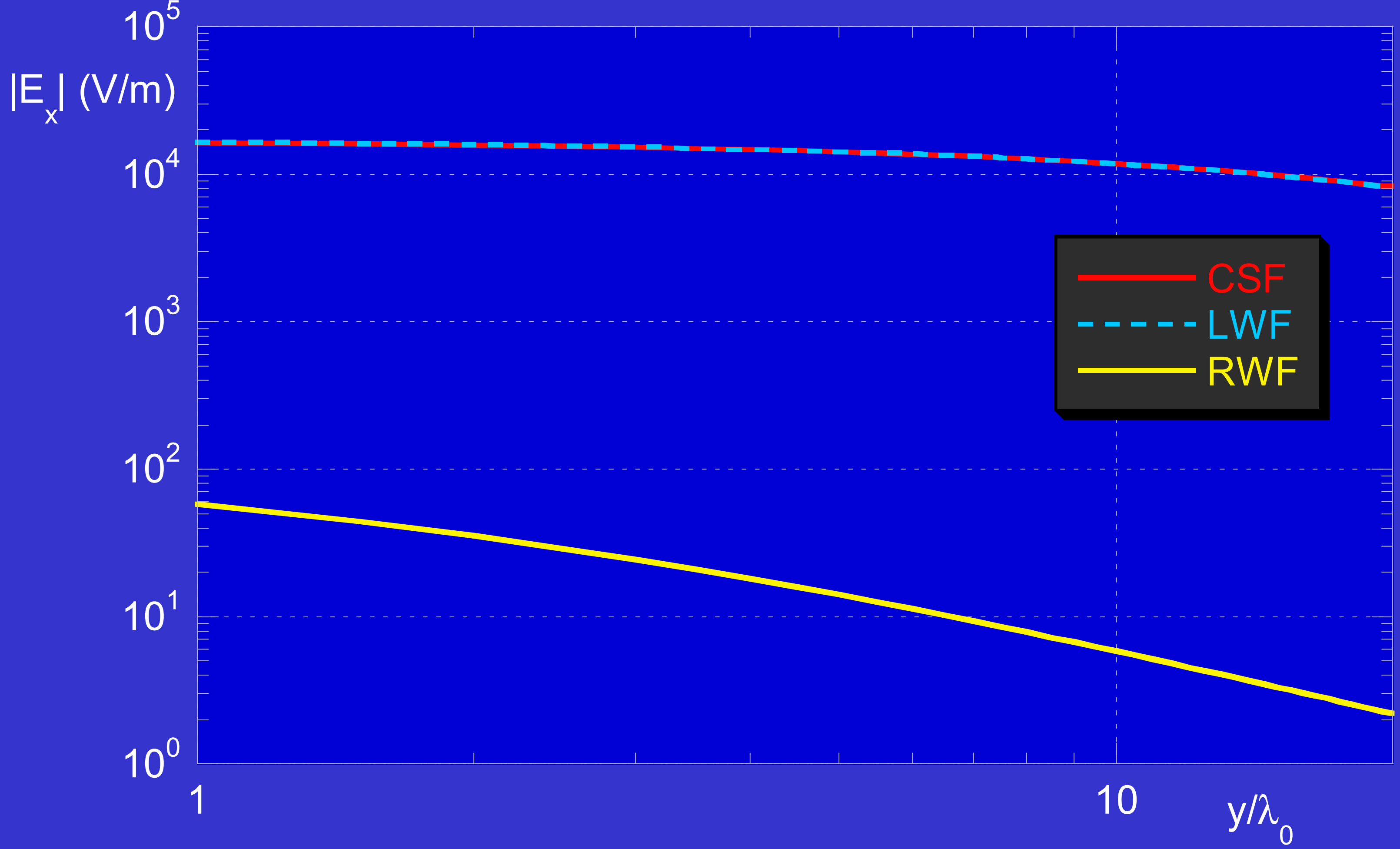

The LWF is an excellent representation of the CSF while the RWF is negligible

Radiation Patterns

f = 30 GHz, $h_s = b/2$

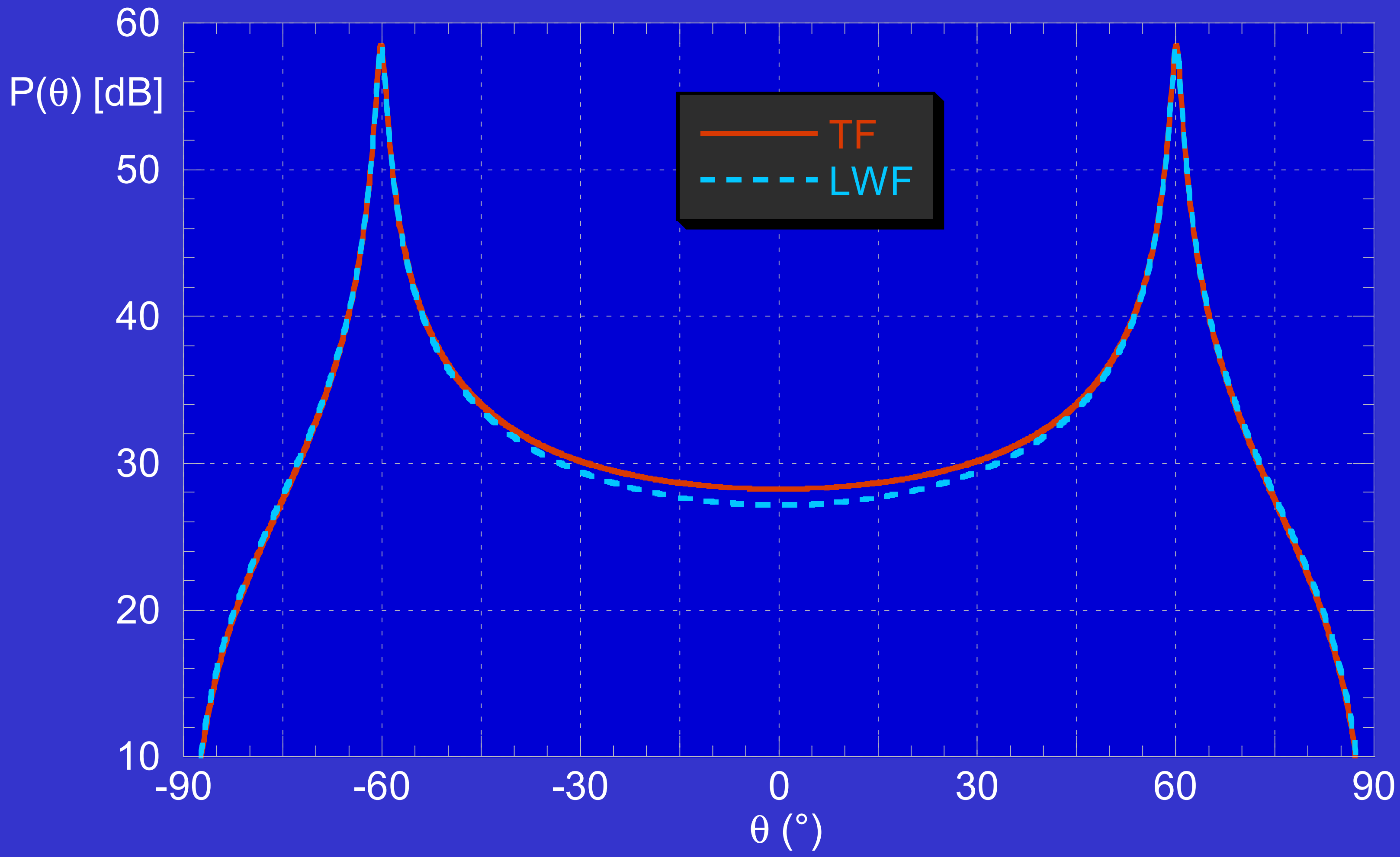

The TF and the LWF are in excellent agreement in the whole elevation plane

Aperture Constituent Fields

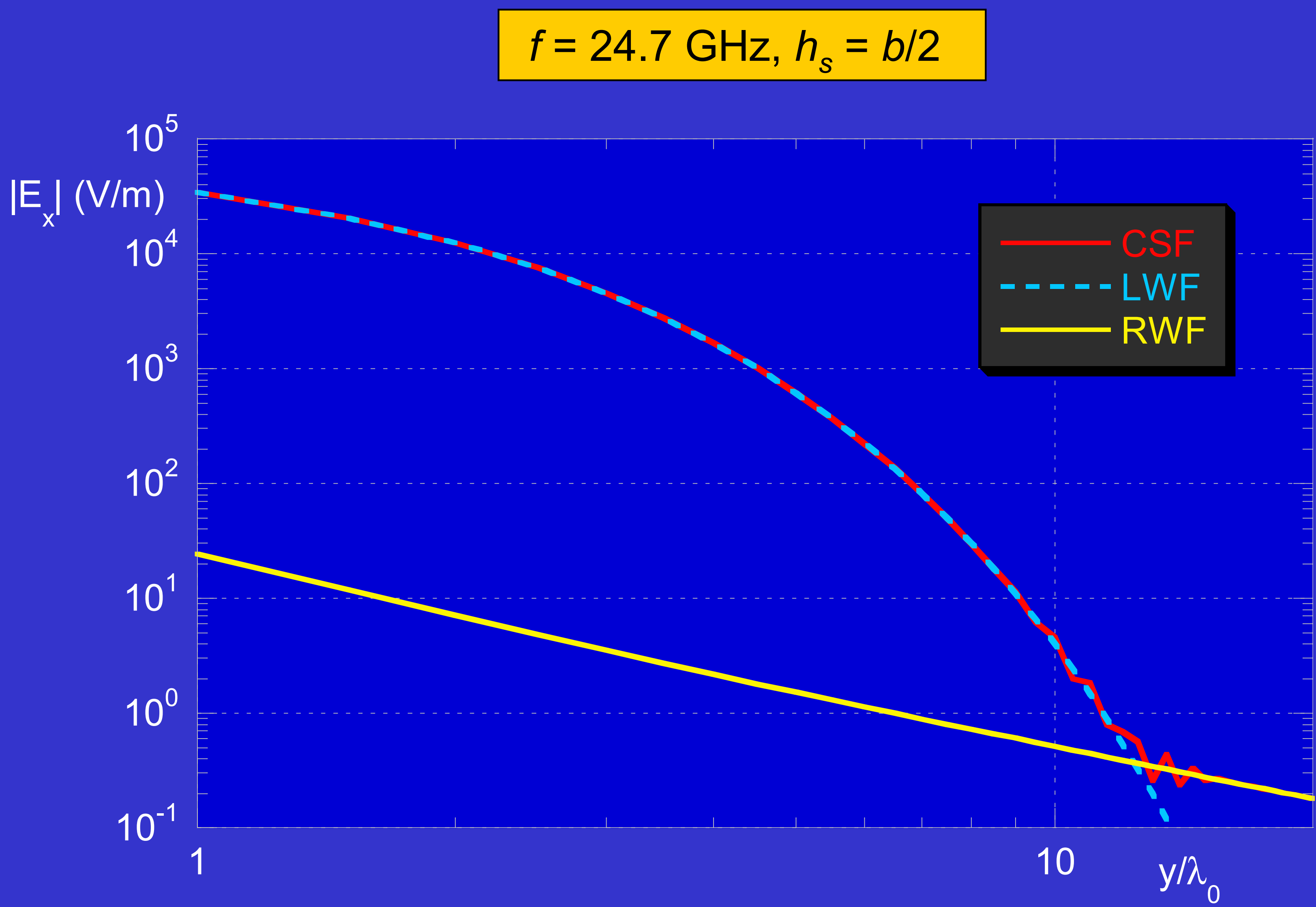

The LWF still dominates the radiative part of the aperture field, although the RWF is the asymptotic dominant contribution

Radiation Patterns

f = 24.7 GHz, $h_s = b/2$

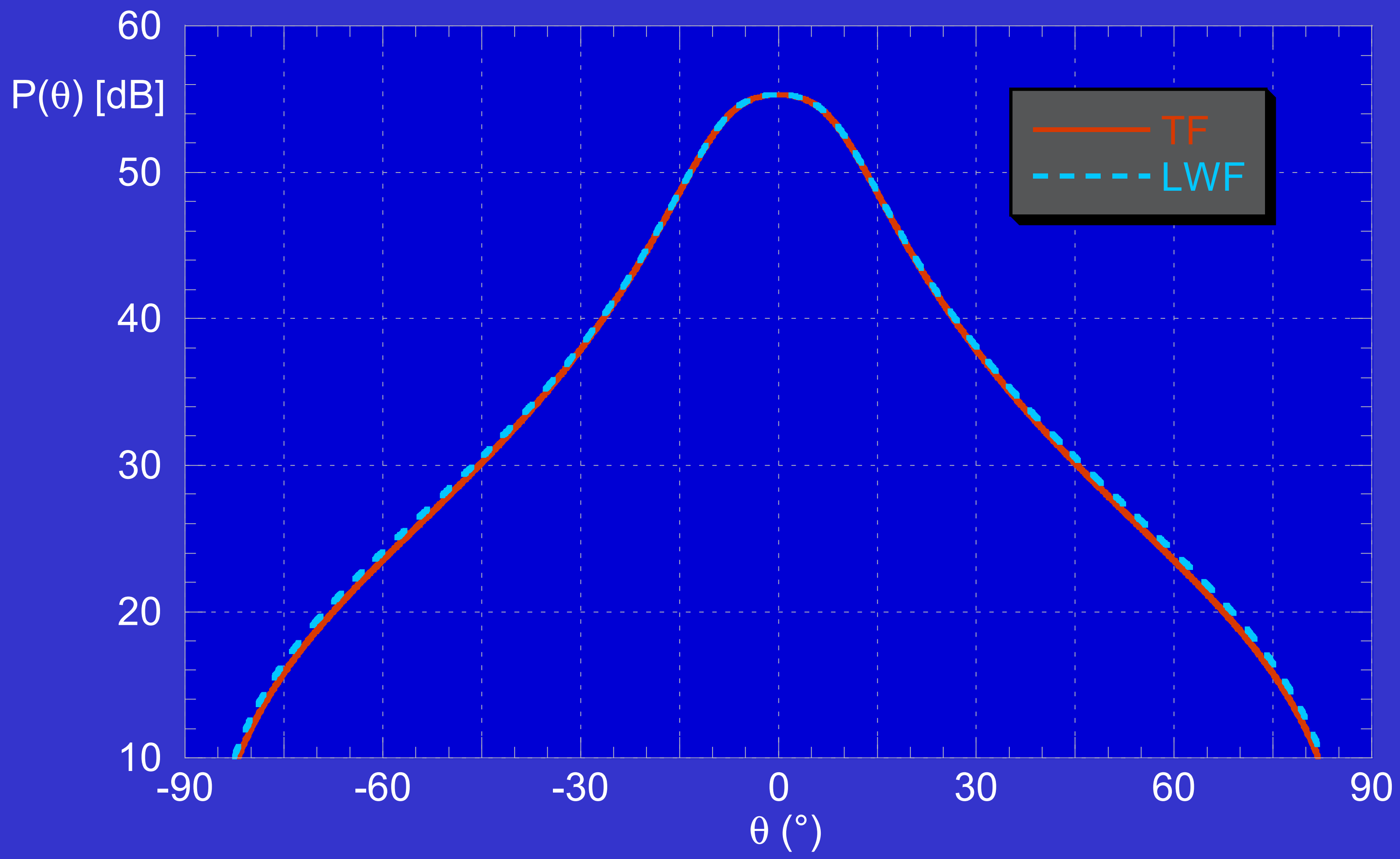

The TF and the LWF are still in excellent agreement in the whole elevation plane

Conclusions

- Radiation characteristics of 1D planar LWAs have been examined
- As an example, a substrate-superstrate structure excited by an electric line source has been studied
- By properly choosing the layer thicknesses this structure acts as a LWA due to the propagation of the TE_3 leaky mode and radiates a narrow-beam pattern at any specified angle
- Numerical results for the dispersion curves, the near and the far field have been provided

Two-Dimensional Uniform Planar Leaky-Wave Antennas

Planar 2D Leaky-Wave Antennas

General form: a partially reflecting surface (PRS) mounted on top of a ground substrate

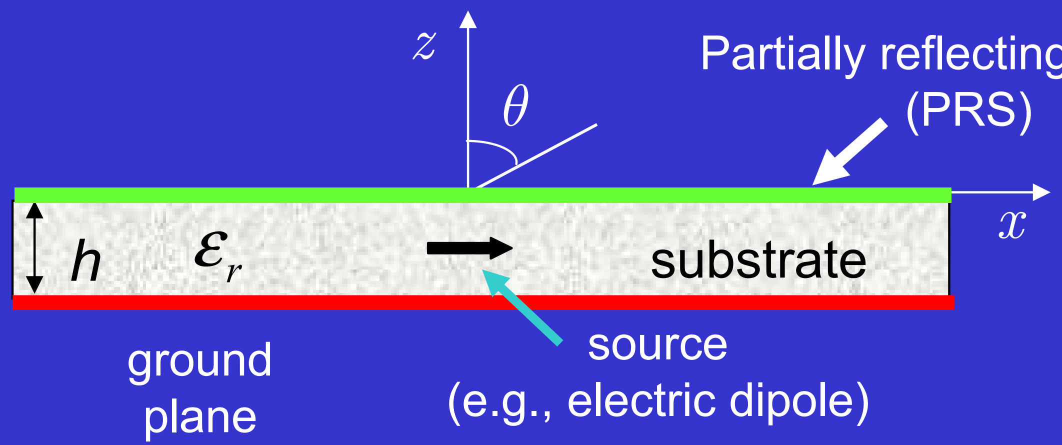

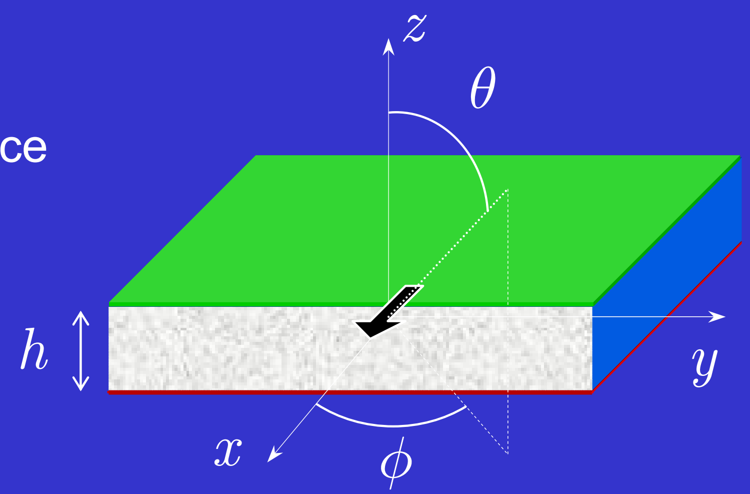

- The source excitation is a simple horizontal dipole located within the substrate, although the pattern mainly depends on the LWA structure and not on the source
- The substrate thickness *h* controls the beam angle
- The PRS controls the beamwidth

Partially Reflecting Surface (PRS)

Fundamental assumption:

At the air-slab interface we assume the presence of some screen (or structure) that partially shields the slab and can be modeled with a homogeneous PRS

Examples of PRS:

high-permittivity superstrate $\varepsilon_{r2} \gg \varepsilon_{r1}$

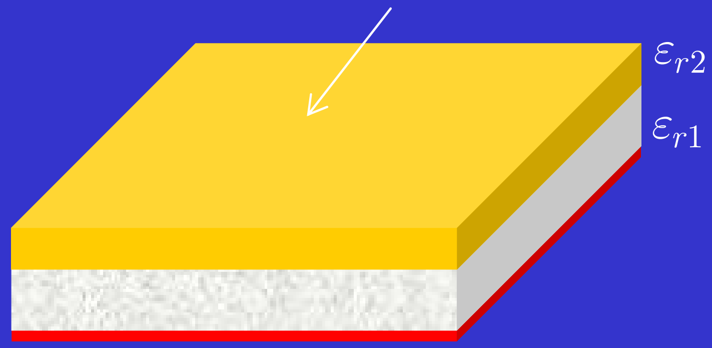

patch (or slot) array

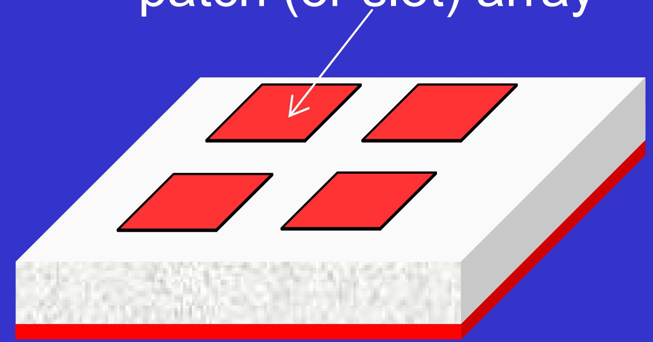

Examples of 2D LWAs with PRS (1)

PRS using a high-permittivity superstrate layer

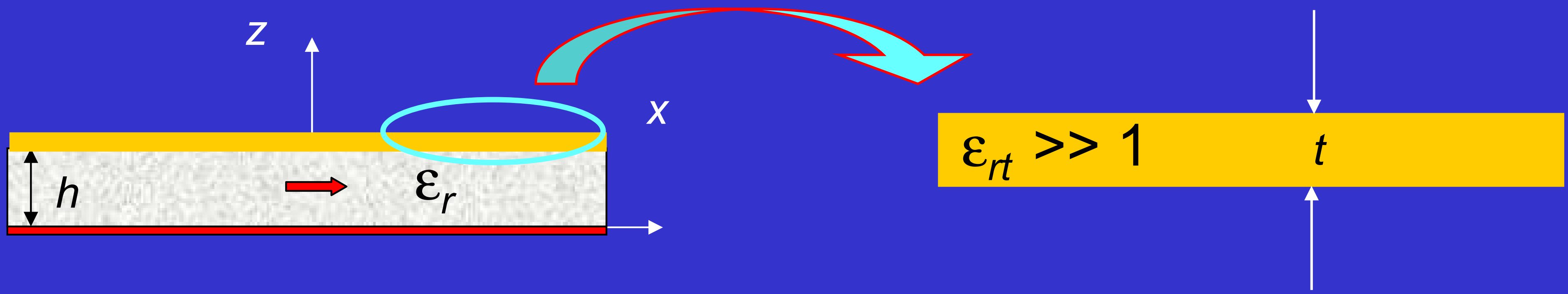

- The PRS is fairly simple
- A higher superstrate permittivity results in a smaller beamwidth
- The PRS is not planar, and may be more expensive

Examples of 2D LWAs with PRS (2)

PRS using metal patches

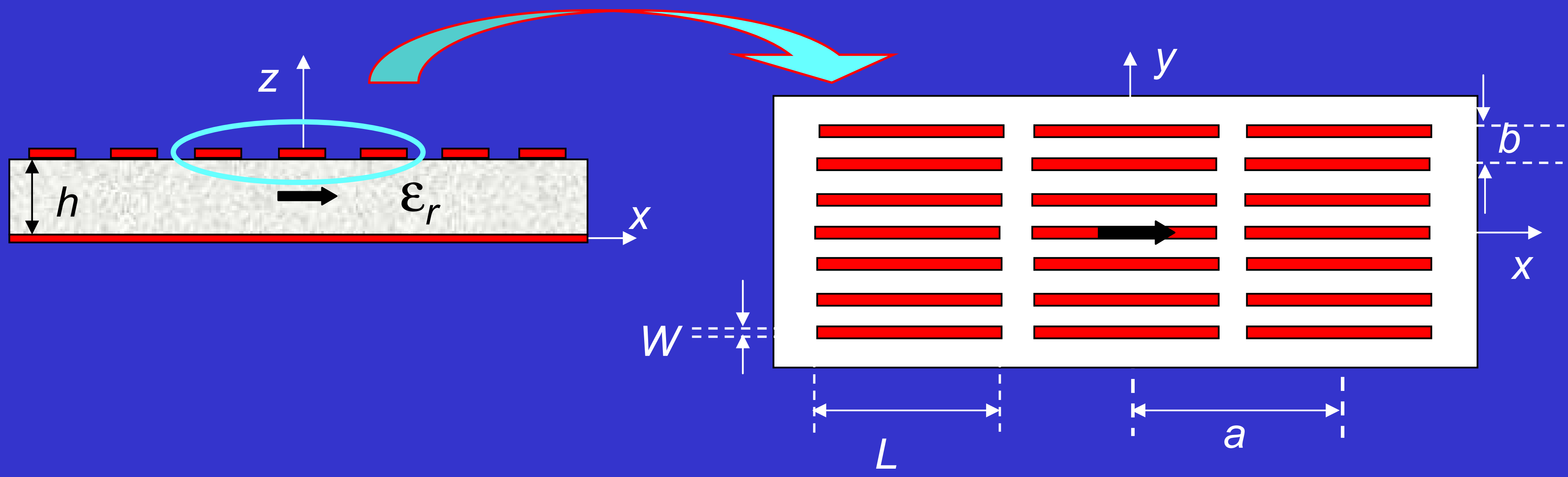

- Larger patches result in a smaller beamwidth
- PRS is simple to etch on PCB

Examples of 2D LWAs with PRS (3)

PRS using slots in metal sheet

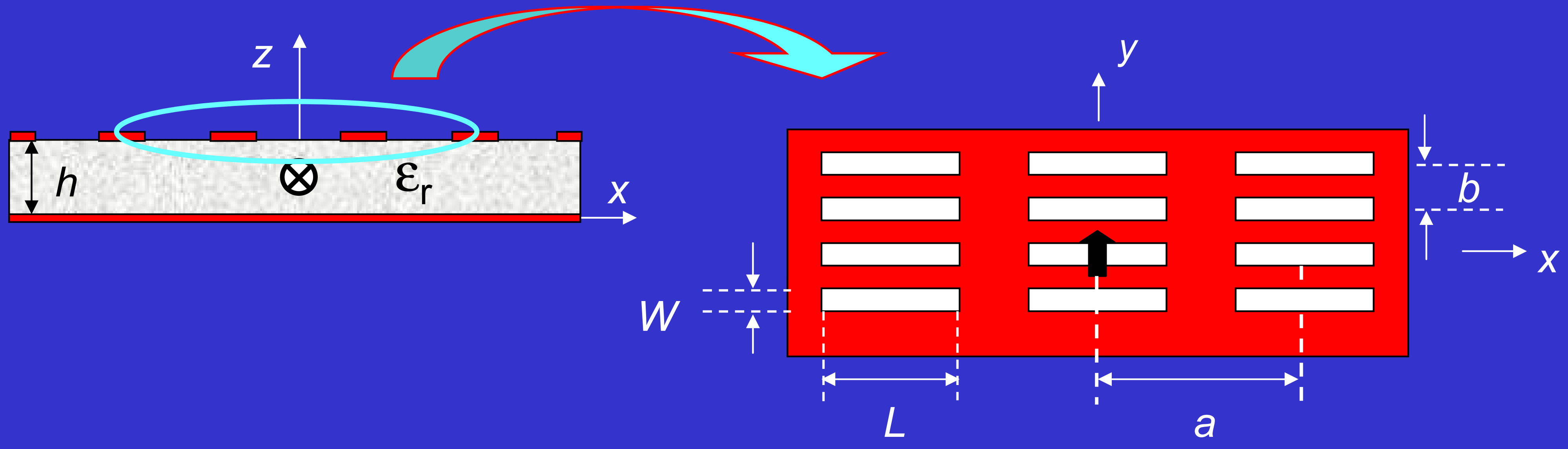

- Smaller slots result in a smaller beamwidth
- PRS is simple to etch on PCB

Basic Principle of Operation (1)

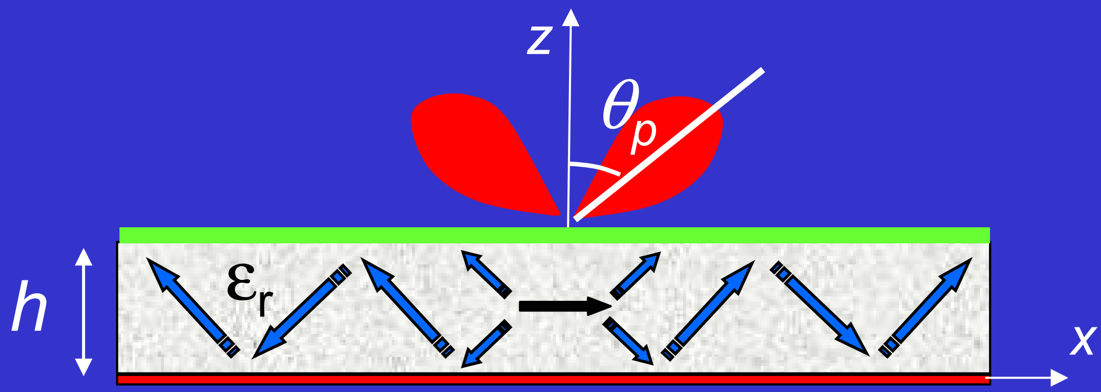

- The PRS partially shields the slab allowing radiation to occur
- The PRS creates a leaky parallel-plate waveguide (PPW) region, which is excited from the source
- The source launches the first higher-order TE and/or TM PPW modes (depending on the source), which are *leaky modes*, due to the PRS

In this class of structures radiation occurs from the *fast-wave* nature of the PPW modes, and not from a space harmonic, and thus the structure is classified as a uniform type of a LWA structure

Basic Principle of Operation (2)

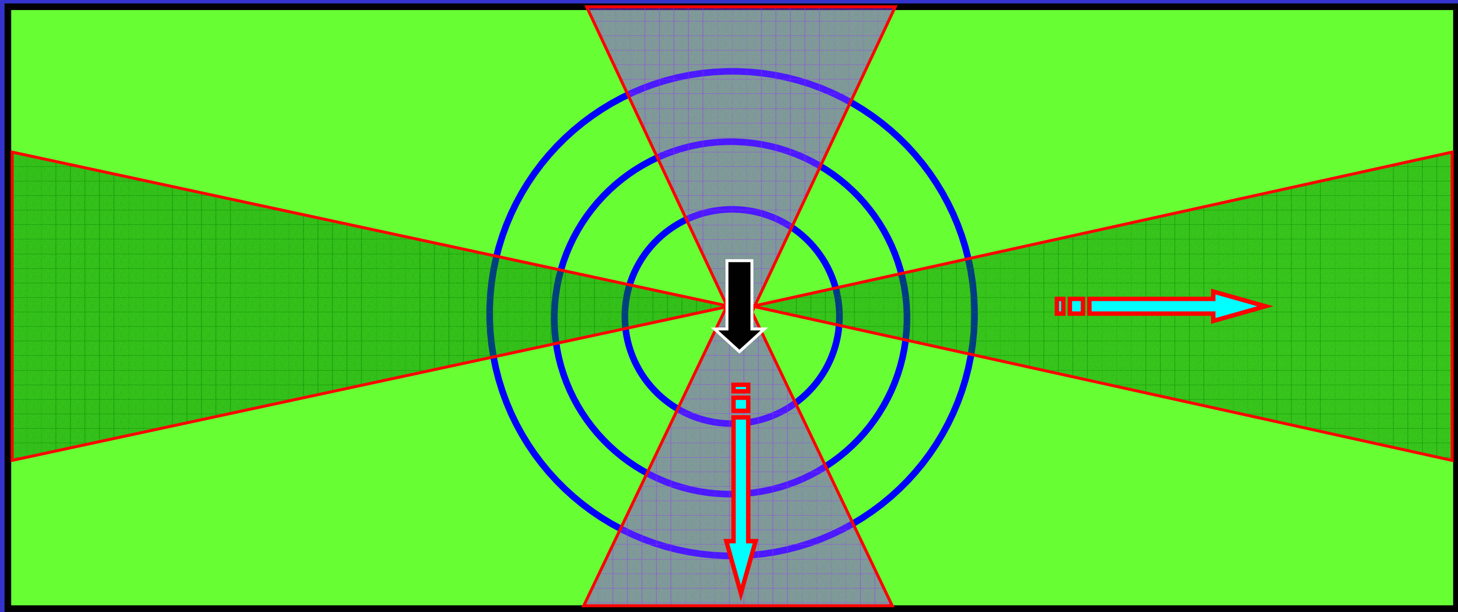

TE$_z$

$$H_z^{TE} \propto A_{TE} \sin\phi$$

TM$_z$

$$E_z^{TM} \propto A_{TM} \cos\phi$$

- The TM$_z$ mode mainly determines the E-plane pattern
- The TE$_z$ mode mainly determines the H-plane pattern

Transverse Equivalent Network (TEN) Model

A transverse equivalent network is used as model of such an antenna

A shunt admittance is used to represent the screen characteristics

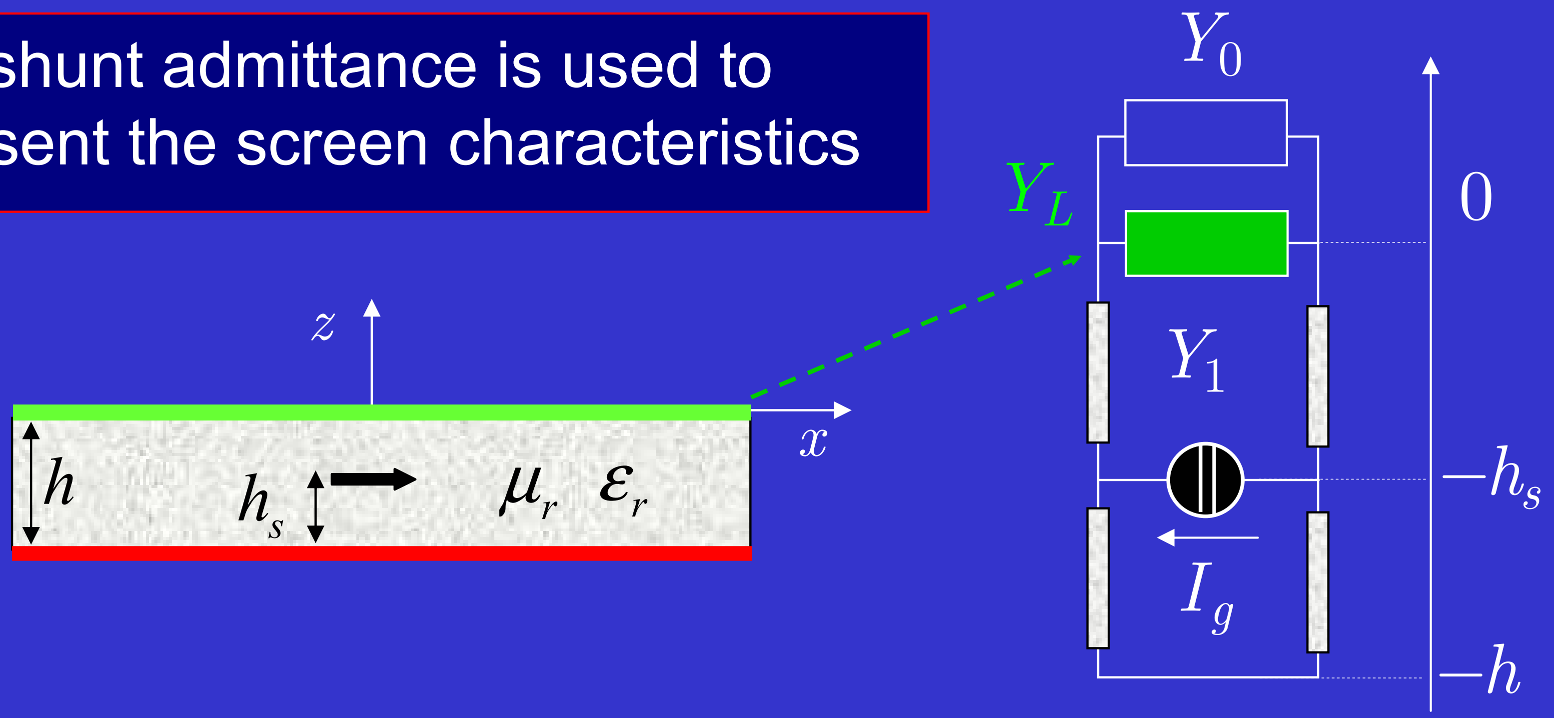

$$Y_0^{TE} = \frac{k_{z0}}{k_0 \eta_0}, \qquad Y_1^{TE} = \frac{k_{z1}}{k_0 \eta_0 \mu_r}$$

$$Y_1^{TM} = \frac{k_0}{\eta_0 k_{z0}}, \qquad Y_1^{TM} = \frac{k_0 \varepsilon_r}{\eta_0 k_{z1}}$$

$$k_{z0} = \sqrt{k_0^2 - k_t^2}$$

$$k_{z1} = \sqrt{k_0^2 \mu_r \varepsilon_r - k_t^2}$$

Far-Field Pattern Calculation (1)

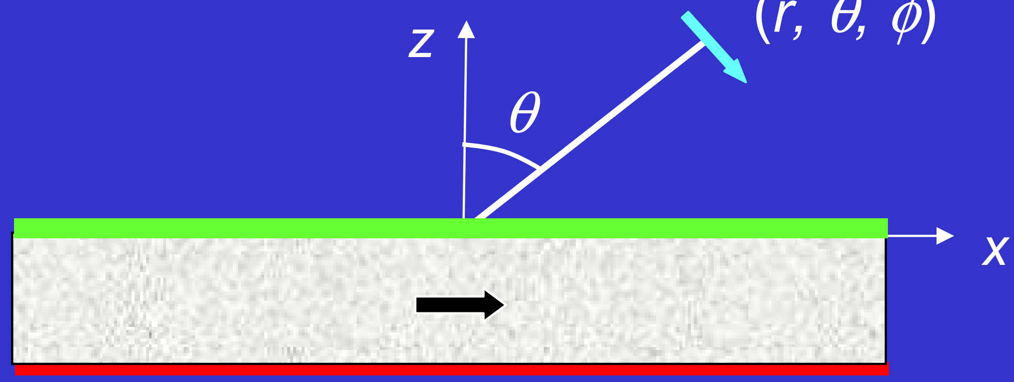

- Reciprocity is used to calculate the far-field pattern (this avoids a calculation of the exact near field and reduce the far-field calculation to one of a plane-wave excitation on the structure)

- A "testing" dipole is placed at the observation point in the θ_0 or ϕ_0 direction. By reciprocity, the field at the observation point is the same at the source dipole location due to the incident wave from the testing dipole (which may be taken as a plane wave due to the far-field location of the testing dipole)

- In the TEN model, the field inside the substrate due to the plane-wave incidence is calculated by finding the voltage on an equivalent transmission-line model (voltage represents the transverse electric field)

Far-Field Pattern Calculation (2)

From reciprocity, the far-field components E_θ and E_ϕ correspond to an ***E*** field from the testing source which is in the plane of incidence and normal to the plane of incidence, respectively

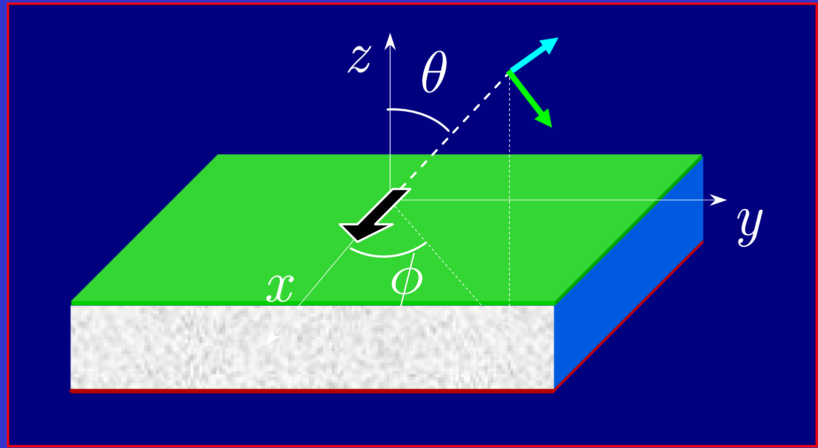

- E_θ is given by $V(-h_s)$ (the voltage at $z = -h_s$ in the TM TEN model due to an incident voltage $V_{inc} = E_0 \cos\theta \cos\phi$)

- E_ϕ is given by $V(-h_s)$ (the voltage at $z = -h_s$ in the TE TEN model due to an incident voltage $V_{inc} = E_0 \sin\phi$)

and where $E_0 = -j\omega\mu_0 \dfrac{e^{-jk_0 r}}{4\pi r}$

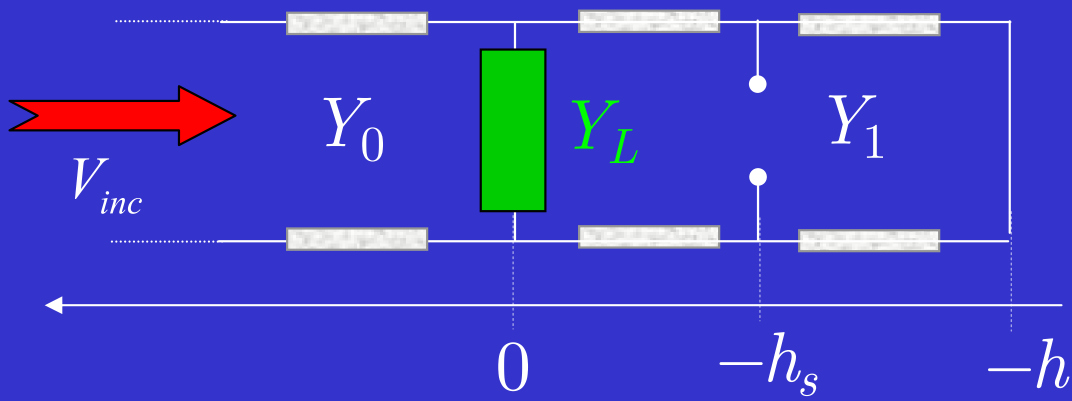

Far-Field Expressions

Assuming a lossless PRS → $Y_L = jB_L$

$$E_\theta = \frac{2E_0 \overline{Y}_0^{TM} \sin(k_{z1}h_s)\cos\theta}{\overline{Y}_0^{TM} \sin(k_{z1}h) + j[\overline{B}_L \sin(k_{z1}h) - \overline{Y}_1^{TM} \cos(k_{z1}h)]}$$

for E-plane $\phi = 0^{o}$

$$E_\phi = \frac{2E_0 \overline{Y}_0^{TE} \sin(k_{z1}h_s)}{\overline{Y}_0^{TE} \sin(k_{z1}h) + j[\overline{B}_L \sin(k_{z1}h) - \overline{Y}_1^{TE} \cos(k_{z1}h)]}$$

for H-plane $\phi = 90^{o}$

$$k_{z1} = k_0\sqrt{n_1^2 - \sin^2\theta} \qquad n_1 = \sqrt{\varepsilon_r} \qquad \overline{B}_L = B_L\eta_0$$

$$\overline{Y}_0^{TM} = \frac{1}{\cos\theta} \qquad \overline{Y}_0^{TE} = \cos\theta$$

$$\overline{Y}_1^{TM} = \frac{\varepsilon_r}{\sqrt{n_1^2 - \sin^2\theta}} \qquad \overline{Y}_1^{TE} = \sqrt{n_1^2 - \sin^2\theta}$$

General Formulas for 2D LWAs

From the closed-form expressions for the far-field pattern of a general 2D LWA, results can be obtained for

- peak-field value
- beamwidth
- pattern bandwidth

Hyp.

If PRS is close to a PEC: $k_{z1}h \approx \pi$ near the peak of the beam

$\left|\bar{B}_L\right| \gg 1$ (corresponding to a narrow-beam LWA)

Peak-Field Expressions

Assuming $h_s = h/2$ (the most usual case):

	E-plane	H-plane
General scan case	$\dfrac{2E_0\left\|\bar{B}_L\right\|}{n_1^2}\sqrt{n_1^2-\sin^2\theta}\cos\theta$	$\dfrac{2E_0\left\|\bar{B}_L\right\|}{\sqrt{n_1^2-\sin^2\theta}}$
Broadside	$\dfrac{2E_0\left\|\bar{B}_L\right\|}{n_1}$	$\dfrac{2E_0\left\|\bar{B}_L\right\|}{n_1}$
Endfire	$\dfrac{2E_0\sqrt{n_1^2-1}}{n_1^2}$	$\dfrac{2E_0\left\|\bar{B}_L\right\|}{\sqrt{n_1^2-1}}$

The peak-field value increases with angle θ_0 in the H-plane, whereas in the E-plane the trend is opposite

The larger the scan angle, the greater the difference between the peak-field values in the E- and H-planes

Beamwidth Expressions

	E-plane	H-plane
General Scan case	$\dfrac{2n_1^{\,2}\sqrt{n_1^{\,2}-\sin^2\theta}}{\pi\,\overline{B}_L^2\sin\theta\cos^2\theta}$	$\dfrac{2\left(\sqrt{n_1^{\,2}-\sin^2\theta}\right)^3}{\pi\,\overline{B}_L^2\sin\theta}$
Broadside	$2\sqrt{\dfrac{2n_1^{\,3}}{\pi\overline{B}_L^2}}$	$2\sqrt{\dfrac{2n_1^{\,3}}{\pi\overline{B}_L^2}}$
Endfire	Narrow beam not possible	$\dfrac{2\left(\sqrt{n_1^{\,2}-1}\right)^3}{\pi\overline{B}_L^2}$

- In the H-plane beamwidth decreases with increasing scan angle
- In the E-plane beamwidth decreases at first as the beam is scanned away from broadside, but then increases with increasing scan angle. A narrow beam at endfire is not possible

3-dB Pattern Bandwidth

Defined as the frequency difference $\Delta f = f_2 - f_1$, where f_1 and f_2 are the frequencies for which the field magnitude at the peak angle θ_0 drops by one half from the value at the center frequency (which gives a peak at θ_0):

	E-plane	H-plane
General Scan case	$\dfrac{2n_1^{\,2}\sec\theta}{\pi \bar{B}_L^2 \sqrt{n_1^{\,2}-\sin^2\theta}}$	$\dfrac{2\sqrt{n_1^{\,2}-\sin^2\theta}}{\pi \bar{B}_L^2 \sec\theta}$
Broadside	$\dfrac{2n_1}{\pi \bar{B}_L^2}$	$\dfrac{2n_1}{\pi \bar{B}_L^2}$
Endfire	0	0

Pattern bandwidth is always inversely related to beamwidth

Effects of the PRS

As $\overline{B}_L$ increases:
- peak-field levels increase
- beams become narrower
- pattern bandwidths decrease

Beamwidth shows a different behavior between the broadside and the scanned cases:

$$\Delta\theta^{scan} \propto \frac{1}{\overline{B}_L^2} \qquad \Delta\theta^{broadside} \propto \frac{1}{\overline{B}_L}$$

For the pattern bandwidth: $\Delta f^{scan/broadside} \propto \dfrac{1}{\overline{B}_L^2}$

There is always a trade-off between beamwidth and pattern bandwidth when designing the antenna

Calculation of Y_L

- The reflection coefficients $\Gamma_{TM}(\theta)$ and $\Gamma_{TE}(\theta)$ are obtained for either E- or H-plane plane-wave incidence on the PRS when it is suspended at an interface between air and a semi-infinite dielectric region

- For a PRS consisting of a periodic structure, this requires a periodic moment method calculation

- From the circuit model

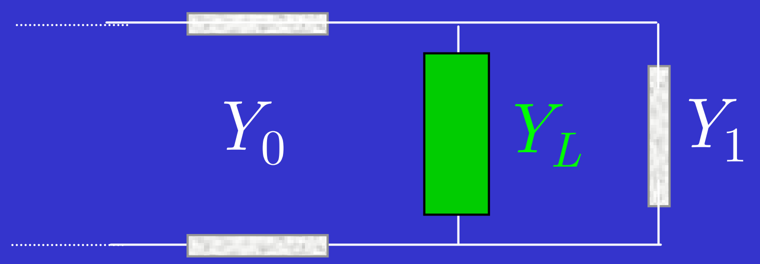

and simple transmission-line theory, the load admittance is obtained

- For example, for the TM case:

$$Y_L^{TM} = Y_0^{TM} \frac{1-\Gamma_{TM}}{1+\Gamma_{TM}} - Y_1^{TM}$$

Example of PRS: Periodic Slotted Screen

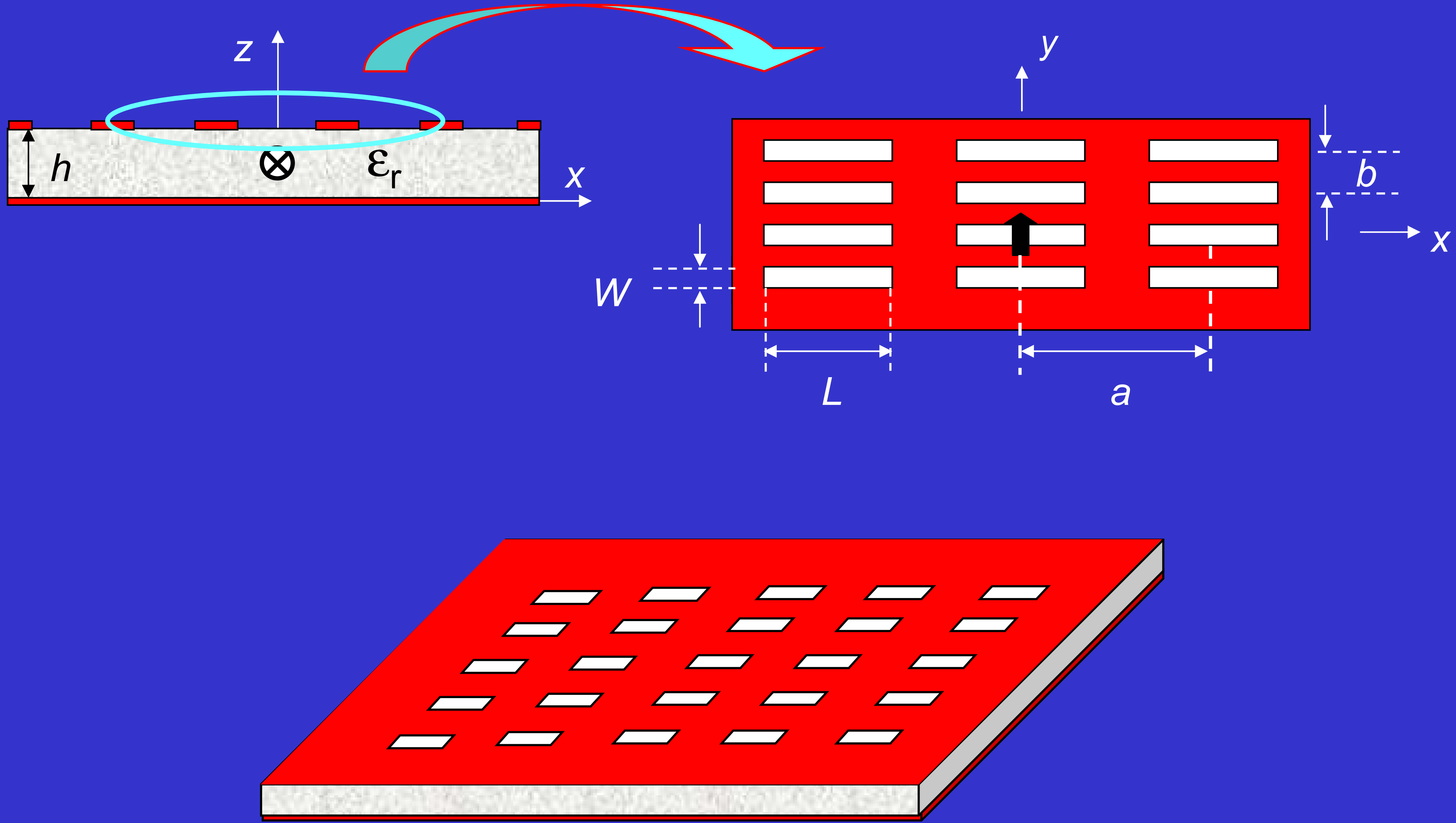

Shunt Admittance vs. Beam Angle

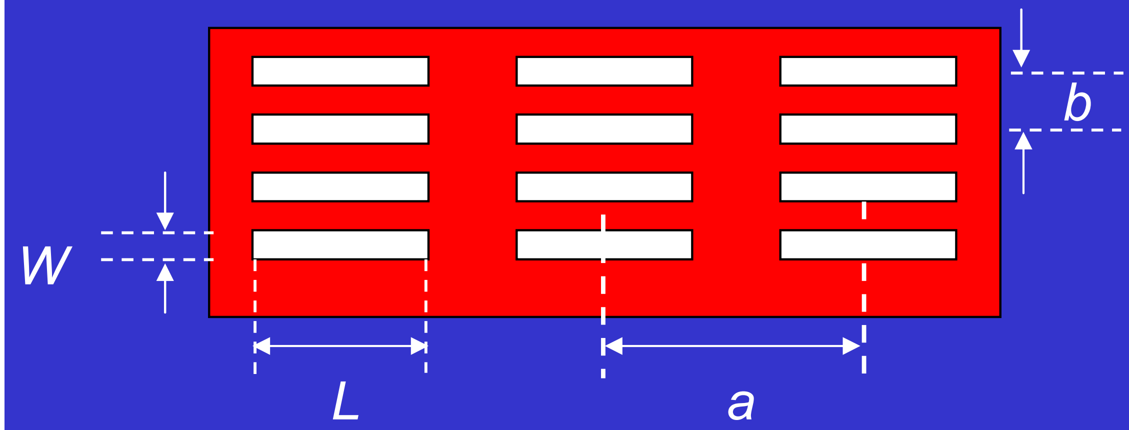

f = 12 GHz
L = 0.6 cm, W = 0.05 cm
a = 1.0 cm, b = 0.3 cm
ε_r = 2.2

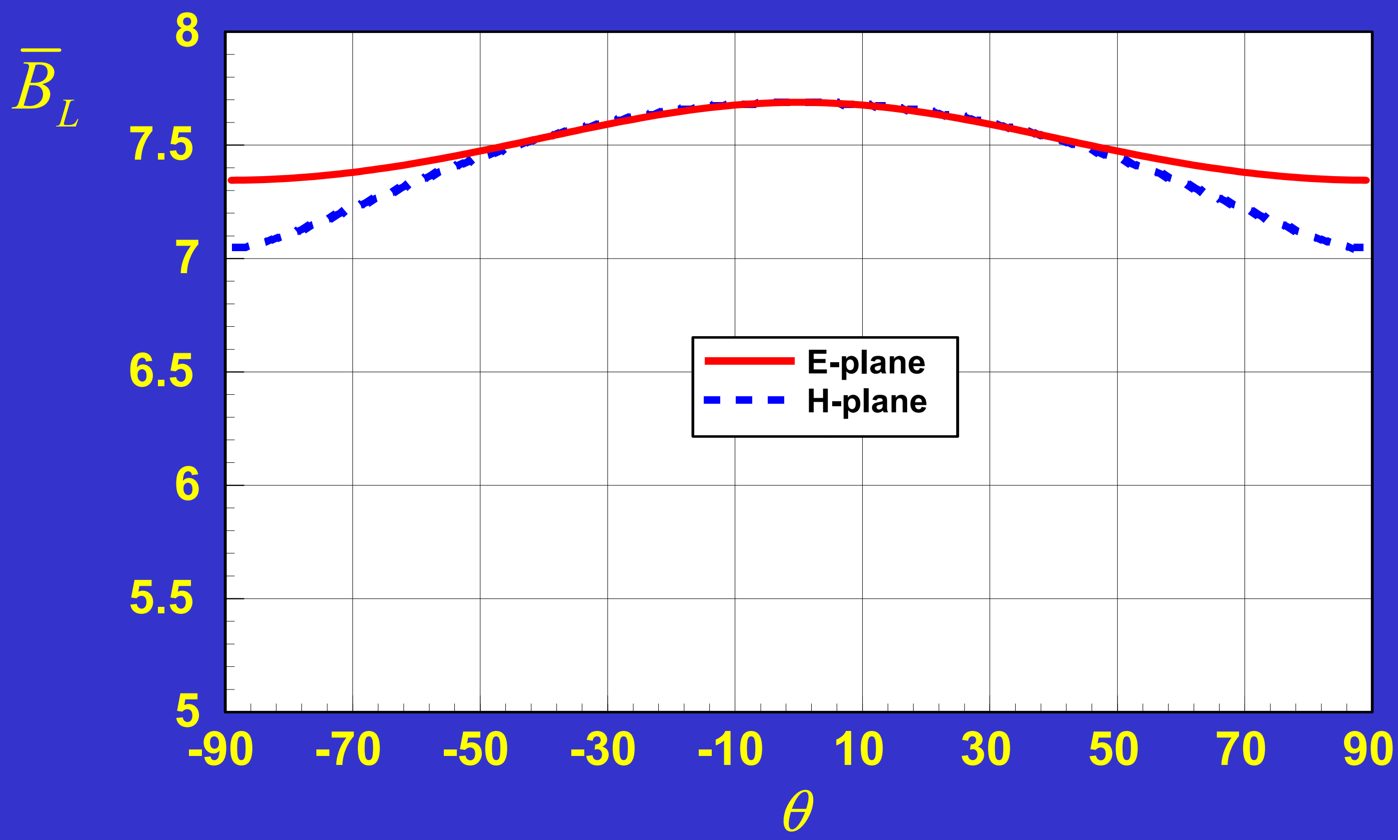

Validation of the Model

- To check the accuracy of the model, results from the TEN model are compared with results from an accurate pattern calculation

- The accurate pattern calculation also uses reciprocity, but, instead of using a simple transmission-line model, a numerically exact spectral domain periodic moment method code is employed

- In the numerically exact approach, the interactions of all the higher order Floquet waves between the screen and the ground plane are accounted for

- Approximate results for normalized peak-field values, beamwidths, and pattern bandwidths obtained by using the general formulas show a very good agreement with the exact results

Example of Patterns: $\theta_p = 45^o$

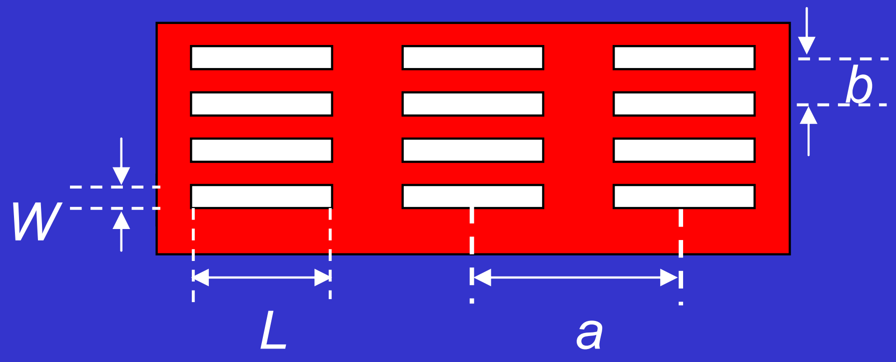

f = 12 GHz
L = 0.6 cm, W = 0.05 cm
a = 1.0 cm, b = 0.3 cm
ε_r = 2.2

h = 1.9 cm

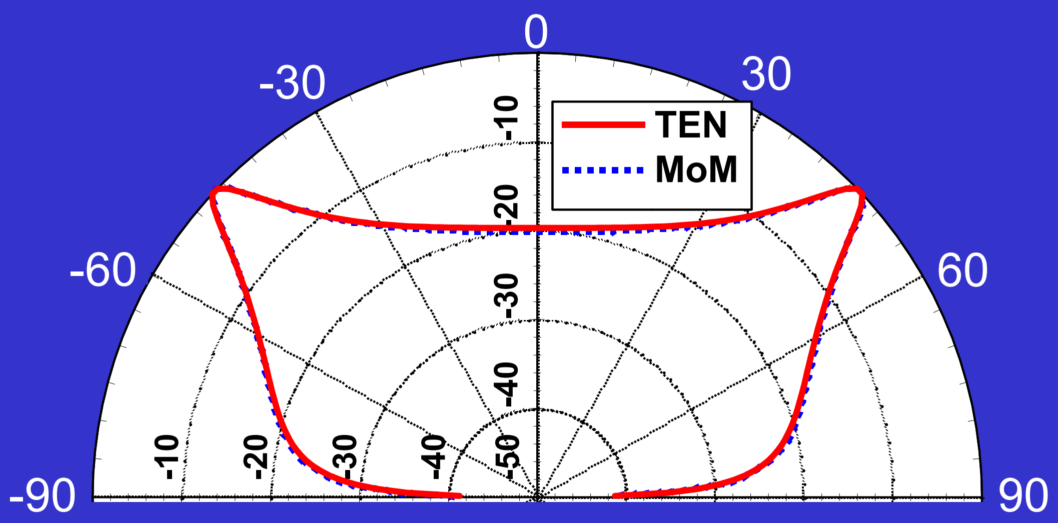

E-plane

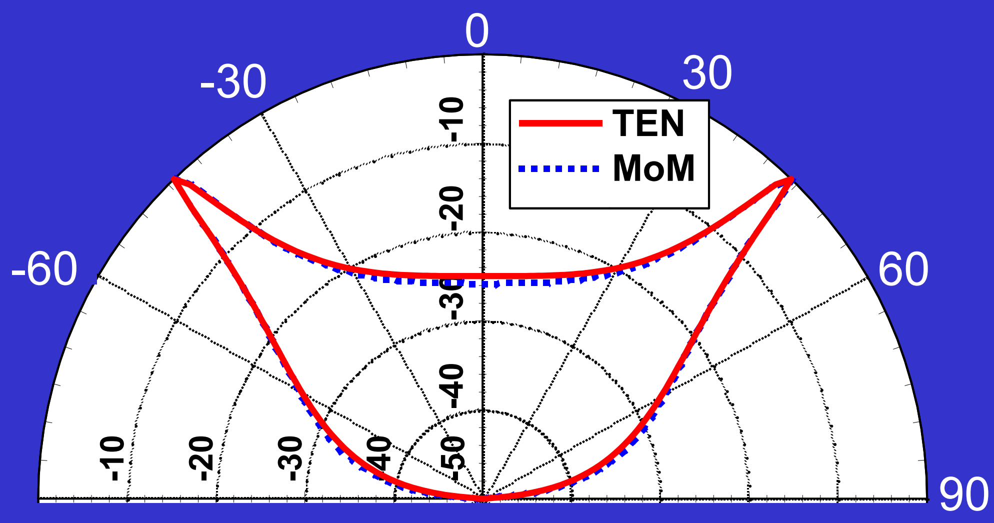

H-plane

Example of Patterns: $\theta_p = 0^o$

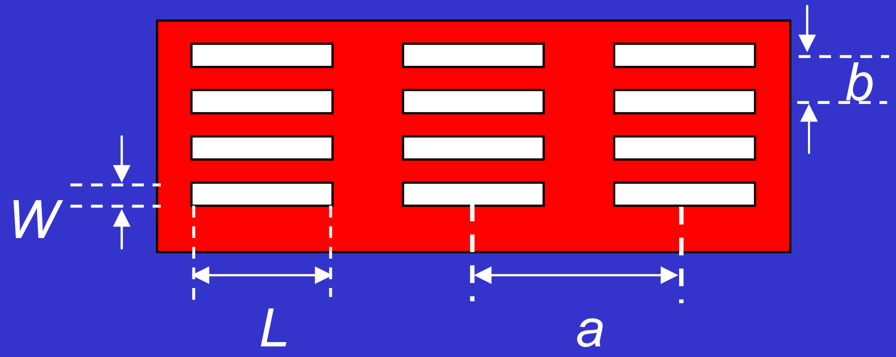

f = 12 GHz
L = 0.6 cm, W = 0.05 cm
a = 1.0 cm, b = 0.3 cm
ε_r = 2.2

h = 1.33 cm

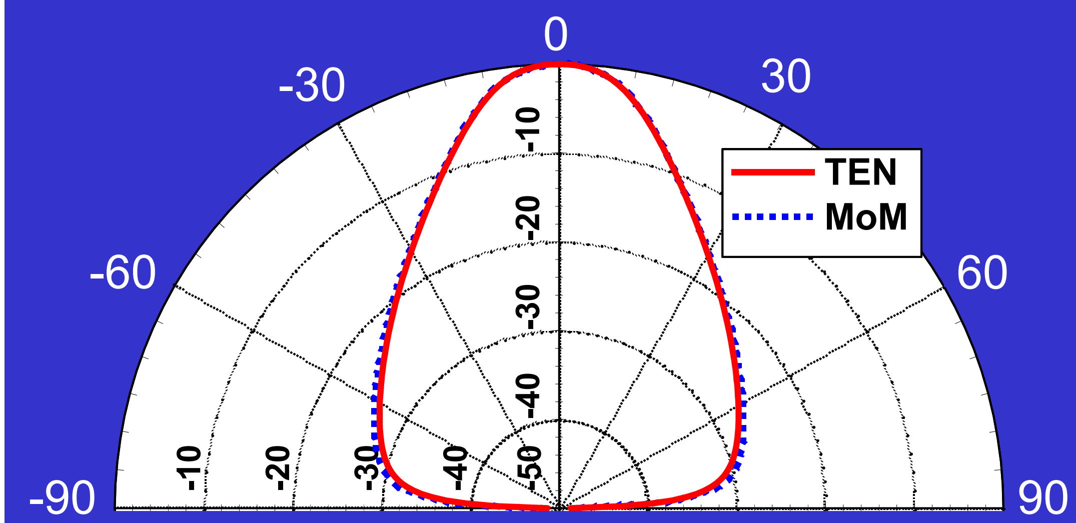

E-plane

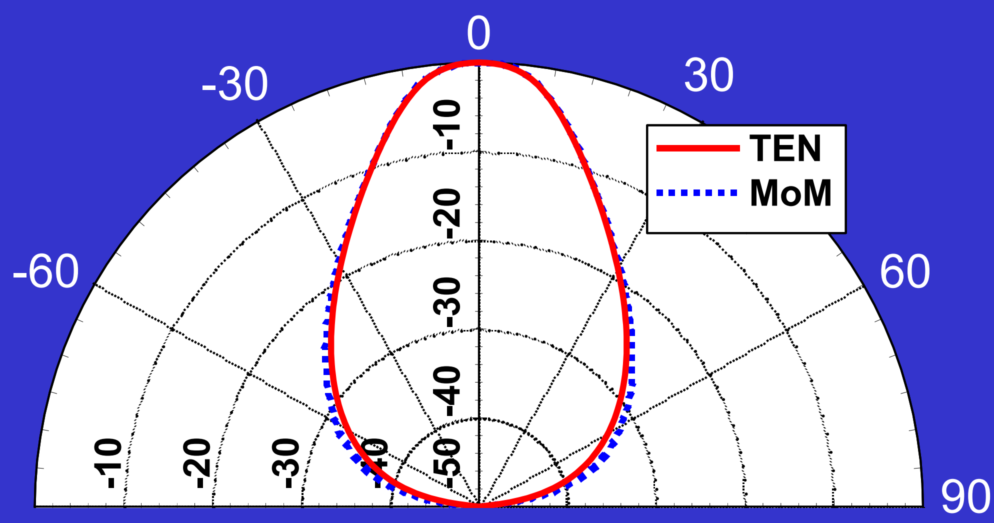

H-plane

Conclusions (1)

- Radiation characteristics of 2D planar LWAs have been examined

- A grounded substrate with a partially reflecting surface (PRS) makes an attractive leaky-wave antenna at high frequencies

- General formulas for the radiation pattern, the peak-field value, the beamwidth and the pattern bandwidth in both the principal planes have been derived, based on a simple transverse equivalent network model

Conclusions (2)

- Numerical results have been shown for one particular type of 2D LWAs, where the PRS is composed of a periodic array of slots in a conducting plane

- A comparison with numerically exact results shows that closed-form expressions are very accurate, with the accuracy increasing as the beamwidth decreases

- The general formulas demonstrate the basic physical properties that are common to all the 2D LWAs

- A symmetric pencil beam can be produced at broadside and narrow-beam scanning is possible down to endfire

References **(1)**

A. Hessel, General characteristics of traveling-wave antennas, in R. E. Collin and F. J. Zucker (Eds.), *Antenna theory*, New York: McGraw-Hill, 1969.

T. Tamir, Leaky-Wave Antennas, in R. E. Collin and F. J. Zucker (Eds.), *Antenna Theory*, New York: McGraw-Hill, 1969.

A. A. Oliner, Leaky-Wave Antennas, in R. C. Johnson (Ed.), *Antenna Engineering Handbook*, New York: McGraw-Hill, 1993.

References (2)

T. Tamir and A. A. Oliner, “Guided complex waves. Part I: Fields at an interface. Part II: Relation to radiation patterns,” *Proc. Inst. Elect. Eng*., vol. 110, pp. 310-334, Feb. 1963.

D. R. Jackson and N. G. Alexòpoulos, “Gain enhancement methods for printed circuit antennas,” *IEEE Trans. Antennas Propagat*., vol. AP-33, pp. 976-987, Sept. 1985.

D. R. Jackson and A. A. Oliner, “A leaky-wave analysis of the high-gain printed antenna configuration,” *IEEE Trans. Antennas Propagat*., vol. 36, pp. 905-910, July 1988.

H. Ostner, J. Detlefsen, and D. R. Jackson, “Radiation from one-dimensional dielectric leaky-wave antennas,” *IEEE Trans. Antennas Propagat*., vol. AP-43, pp. 331-339, Apr. 1995.

References (3)

A. Ip and D. R. Jackson, “Radiation from cylindrical leaky waves,” *IEEE Trans. Antennas Propagat*., vol. 38, pp. 482-488, Apr. 1990.

D. R. Jackson, A. A. Oliner, and A. Ip, “Leaky-wave propagation and radiation for a narrow-beam multiple-layer dielectric structure,” *IEEE Trans. Antennas Propagat*., vol. AP-41, pp. 344-348, Mar. 1993.

T. Zhao, D. R. Jackson, J. T. Williams, and A. A. Oliner, “General formulas for a 2D leaky-wave antenna,” *IEEE Digest AP-S Int. Symp.* 2003, vol. 2, Columbus, OH, pp. 1134-1137, June 2003.

T. Zhao, D. R. Jackson, and J. T. Williams, “Radiation characteristics of a 2D periodic leaky-wave antenna using metal patches or slots,” *IEEE Digest AP-S Int. Symp. 2001*, vol. 3, Boston, MA, pp. 260-263, July 2001.

T. Zhao, D. R. Jackson, J. T. Williams, and A. A. Oliner, “Simple CAD model for a dielectric leaky-wave antenna,” *IEEE Antennas Wireless Propagat. Lett*., vol. 3, pp. 243-245, 2004.

We wish to thank prof. David R. Jackson
for having kindly provided
the material on 2D LWAs presented here

Thank you!